

J/ψ and $\psi(2S)$ Production in $p\bar{p}$ Collisions at $\sqrt{s} = 1.8$ TeV

F. Abe,¹⁶ H. Akimoto,³⁵ A. Akopian,³⁰ M. G. Albrow,⁷ S. R. Amendolia,²⁶ D. Amidei,¹⁹ J. Antos,³² S. Aota,³⁵ G. Apollinari,³⁰ T. Asakawa,³⁵ W. Ashmanskas,¹⁷ M. Atac,⁷ F. Azfar,²⁵ P. Azzi-Bacchetta,²⁴ N. Bacchetta,²⁴ W. Badgett,¹⁹ S. Bagdasarov,³⁰ M. W. Bailey,²¹ J. Bao,³⁸ P. de Barbaro,²⁹ A. Barbaro-Galtieri,¹⁷ V. E. Barnes,²⁸ B. A. Barnett,¹⁵ M. Barone,⁹ E. Barzi,⁹ G. Bauer,¹⁸ T. Baumann,¹¹ F. Bedeschi,²⁶ S. Behrends,³ S. Belforte,²⁶ G. Bellettini,²⁶ J. Bellinger,³⁷ D. Benjamin,³⁴ J. Benlloch,¹⁸ J. Bensinger,³ D. Benton,²⁵ A. Beretvas,⁷ J. P. Berge,⁷ J. Berryhill,⁵ S. Bertolucci,⁹ B. Bevensee,²⁵ A. Bhatti,³⁰ K. Biery,⁷ M. Binkley,⁷ D. Bisello,²⁴ R. E. Blair,¹ C. Blocker,³ A. Bodek,²⁹ W. Bokhari,¹⁸ V. Bolognesi,² G. Bolla,²⁸ D. Bortoletto,²⁸ J. Boudreau,²⁷ L. Breccia,² C. Bromberg,²⁰ N. Bruner,²¹ E. Buckley-Geer,⁷ H. S. Budd,²⁹ K. Burkett,¹⁹ G. Busetto,²⁴ A. Byon-Wagner,⁷ K. L. Byrum,¹ J. Cammerata,¹⁵ C. Campagnari,⁷ M. Campbell,¹⁹ A. Caner,²⁶ W. Carithers,¹⁷ D. Carlsmith,³⁷ A. Castro,²⁴ D. Cauz,²⁶ Y. Cen,²⁹ F. Cervelli,²⁶ P. S. Chang,³² P. T. Chang,³² H. Y. Chao,³² J. Chapman,¹⁹ M.-T. Cheng,³² G. Chiarelli,²⁶ T. Chikamatsu,³⁵ C. N. Chiou,³² L. Christofek,¹³ S. Cihangir,⁷ A. G. Clark,¹⁰ M. Cobal,²⁶ E. Cocca,²⁶ M. Contreras,⁵ J. Conway,³¹ J. Cooper,⁷ M. Cordelli,⁹ C. Couyoumtzelis,¹⁰ D. Crane,¹ D. Cronin-Hennessy,⁶ R. Culbertson,⁵ T. Daniels,¹⁸ F. DeJongh,⁷ S. Delchamps,⁷ S. Dell'Agnello,²⁶ M. Dell'Orso,²⁶ R. Demina,⁷ L. Demortier,³⁰ M. Deninno,² P. F. Derwent,⁷ T. Devlin,³¹ J. R. Dittmann,⁶ S. Donati,²⁶ J. Done,³³ T. Dorigo,²⁴ A. Dunn,¹⁹ N. Eddy,¹⁹ K. Einsweiler,¹⁷ J. E. Elias,⁷ R. Ely,¹⁷ E. Engels, Jr.,²⁷ D. Errede,¹³ S. Errede,¹³ Q. Fan,²⁹ G. Feild,³⁸ C. Ferretti,²⁶ I. Fiori,² B. Flaughner,⁷ G. W. Foster,⁷ M. Franklin,¹¹ M. Frautschi,³⁴ J. Freeman,⁷ J. Friedman,¹⁸ Y. Fukui,¹⁶ S. Funaki,³⁵ S. Galeotti,²⁶ M. Gallinaro,²⁵ O. Ganel,³⁴ M. Garcia-Sciveres,¹⁷ A. F. Garfinkel,²⁸ C. Gay,¹¹ S. Geer,⁷ D. W. Gerdes,¹⁵ P. Giannetti,²⁶ N. Giokaris,³⁰ P. Giromini,⁹ G. Giusti,²⁶ L. Gladney,²⁵ D. Glenzinski,¹⁵ M. Gold,²¹ J. Gonzalez,²⁵ A. Gordon,¹¹ A. T. Goshaw,⁶ Y. Gotra,²⁴ K. Goulianos,³⁰ H. Grassmann,²⁶ L. Groer,³¹ C. Grosso-Pilcher,⁵ G. Guillian,¹⁹ R. S. Guo,³² C. Haber,¹⁷ E. Hafen,¹⁸ S. R. Hahn,⁷ R. Hamilton,¹¹ R. Handler,³⁷ R. M. Hans,³⁸ F. Happacher,⁹ K. Hara,³⁵ A. D. Hardman,²⁸ B. Harral,²⁵ R. M. Harris,⁷ S. A. Hauger,⁶ J. Hauser,⁴ C. Hawk,³¹ E. Hayashi,³⁵ J. Heinrich,²⁵ B. Hinrichsen,¹⁴ K. D. Hoffman,²⁸ M. Hohlmann,⁵ C. Holck,²⁵ R. Hollebeek,²⁵ L. Holloway,¹³ A. Hölscher,¹⁴ S. Hong,¹⁹ G. Houk,²⁵ P. Hu,²⁷ B. T. Huffman,²⁷ R. Hughes,²² J. Huston,²⁰ J. Huth,¹¹ J. Hylen,⁷ H. Ikeda,³⁵ M. Incagli,²⁶ J. Incandela,⁷ G. Introzzi,²⁶ J. Iwai,³⁵ Y. Iwata,¹² H. Jensen,⁷ U. Joshi,⁷ R. W. Kadel,¹⁷ E. Kajfasz,²⁴ H. Kambara,¹⁰ T. Kamon,³³ T. Kaneko,³⁵ K. Karr,³⁶ H. Kasha,³⁸ Y. Kato,²³ T. A. Keaffaber,²⁸ L. Keeble,⁹ K. Kelley,¹⁸ R. D. Kennedy,⁷ R. Kephart,⁷ P. Kesten,¹⁷ D. Kestenbaum,¹¹ R. M. Keup,¹³ H. Keutelian,⁷ F. Keyvan,⁴ B. Kharadia,¹³ B. J. Kim,²⁹ D. H. Kim,^{7,*} H. S. Kim,¹⁴ S. B. Kim,¹⁹ S. H. Kim,³⁵ Y. K. Kim,¹⁷ L. Kirsch,³ P. Koehn,²⁹ K. Kondo,³⁵ J. Konigsberg,⁸ S. Kopp,⁵ K. Kordas,¹⁴ A. Korytov,⁸ W. Koska,⁷ E. Kovacs,^{7,*} W. Kowald,⁶ M. Krasberg,¹⁹ J. Kroll,⁷ M. Kruse,²⁹ T. Kuwabara,³⁵ S. E. Kuhlmann,¹ E. Kuns,³¹ A. T. Laasanen,²⁸ S. Lami,²⁶ S. Lammel,⁷ J. I. Lamoureux,³ T. LeCompte,¹ S. Leone,²⁶ J. D. Lewis,⁷ P. Limon,⁷ M. Lindgren,⁴ T. M. Liss,¹³ Y. C. Liu,³² N. Lockyer,²⁵ O. Long,²⁵ C. Loomis,³¹ M. Loreti,²⁴ J. Lu,³³ D. Lucchesi,²⁶ P. Lukens,⁷ S. Lusin,³⁷ J. Lys,¹⁷ K. Maeshima,⁷ A. Maghakian,³⁰ P. Maksimovic,¹⁸ M. Mangano,²⁶ J. Mansour,²⁰ M. Mariotti,²⁴ J. P. Marriner,⁷ A. Martin,³⁸ J. A. J. Matthews,²¹ R. Mattingly,¹⁸ P. McIntyre,³³ P. Melese,³⁰ A. Menzione,²⁶ E. Meschi,²⁶ S. Metzler,²⁵ C. Miao,¹⁹ T. Miao,⁷ G. Michail,¹¹ R. Miller,²⁰ H. Minato,³⁵ S. Miscetti,⁹ M. Mishina,¹⁶ H. Mitsushio,³⁵ T. Miyamoto,³⁵ S. Miyashita,³⁵ N. Moggi,²⁶ Y. Morita,¹⁶ J. Mueller,²⁷ A. Mukherjee,⁷ T. Muller,⁴ P. Murat,²⁶ H. Nakada,³⁵ I. Nakano,³⁵ C. Nelson,⁷ D. Neuberger,⁴ C. Newman-Holmes,⁷ C.-Y. P. Ngan,¹⁸ M. Ninomiya,³⁵ L. Nodulman,¹ S. H. Oh,⁶ K. E. Ohl,³⁸ T. Ohmoto,¹² T. Ohsugi,¹² R. Oishi,³⁵ M. Okabe,³⁵ T. Okusawa,²³ R. Oliveira,²⁵ J. Olsen,³⁷ C. Pagliarone,² R. Paoletti,²⁶ V. Papadimitriou,³⁴ S. P. Pappas,³⁸ N. Parashar,²⁶ S. Park,⁷ A. Parri,⁹ J. Patrick,⁷ G. Pauletta,²⁶ M. Paulini,¹⁷ A. Perazzo,²⁶ L. Pescara,²⁴ M. D. Peters,¹⁷ T. J. Phillips,⁶ G. Piacentino,² M. Pillai,²⁹ K. T. Pitts,⁷ R. Plunkett,⁷ L. Pondrom,³⁷ J. Proudfoot,¹ F. Ptohos,¹¹ G. Punzi,²⁶ K. Ragan,¹⁴ D. Reher,¹⁷ A. Ribon,²⁴ F. Rimondi,² L. Ristori,²⁶ W. J. Robertson,⁶ T. Rodrigo,²⁶ S. Rolli,³⁶ J. Romano,⁵ L. Rosenson,¹⁸ R. Roser,¹³ T. Saab,¹⁴ W. K. Sakumoto,²⁹ D. Saltzberg,⁵ A. Sansoni,⁹ L. Santi,²⁶ H. Sato,³⁵ P. Schlabach,⁷ E. E. Schmidt,⁷ M. P. Schmidt,³⁸ A. Scribano,²⁶ S. Segler,⁷ S. Seidel,²¹ Y. Seiya,³⁵ G. Sganos,¹⁴ M. D. Shapiro,¹⁷ N. M. Shaw,²⁸ Q. Shen,²⁸ P. F. Shepard,²⁷ M. Shimojima,³⁵ M. Shochet,⁵ J. Siegrist,¹⁷ A. Sill,³⁴ P. Sinervo,¹⁴ P. Singh,²⁷ J. Skarha,¹⁵ K. Sliwa,³⁶ F. D. Snider,¹⁵ T. Song,¹⁹ J. Spalding,⁷ T. Speer,¹⁰ P. Sphicas,¹⁸ F. Spinella,²⁶ M. Spiropulu,¹¹ L. Spiegel,⁷ L. Stanco,²⁴ J. Steele,³⁷ A. Stefanini,²⁶ K. Strahl,¹⁴ J. Strait,⁷ R. Ströhmer,^{7,*} D. Stuart,⁷ G. Sullivan,⁵ K. Sumorok,¹⁸ J. Suzuki,³⁵ T. Takada,³⁵ T. Takahashi,²³ T. Takano,³⁵ K. Takikawa,³⁵ N. Tamura,¹² B. Tannenbaum,²¹ F. Tartarelli,²⁶ W. Taylor,¹⁴ P. K. Teng,³² Y. Teramoto,²³ S. Tether,¹⁸ D. Theriot,⁷

T. L. Thomas,²¹ R. Thun,¹⁹ M. Timko,³⁶ P. Tipton,²⁹ A. Titov,³⁰ S. Tkaczyk,⁷ D. Toback,⁵ K. Tollefson,²⁹ A. Tollestrup,⁷ W. Trischuk,¹⁴ J. F. de Troconiz,¹¹ S. Truitt,¹⁹ J. Tseng,¹⁸ N. Turini,²⁶ T. Uchida,³⁵ N. Uemura,³⁵ F. Ukegawa,²⁵ G. Unal,²⁵ J. Valls,^{7,*} S. C. van den Brink,²⁷ S. Vejck III,¹⁹ G. Velev,²⁶ R. Vidal,⁷ R. Vilar,^{7,*} M. Vondracek,¹³ D. Vucinic,¹⁸ R. G. Wagner,¹ R. L. Wagner,⁷ J. Wahl,⁵ N. B. Wallace,²⁶ A. M. Walsh,³¹ C. Wang,⁶ C. H. Wang,³² J. Wang,⁵ M. J. Wang,³² Q. F. Wang,³⁰ A. Warburton,¹⁴ T. Watts,³¹ R. Webb,³³ C. Wei,⁶ C. Wendt,³⁷ H. Wenzel,¹⁷ W. C. Wester III,⁷ A. B. Wicklund,¹ E. Wicklund,⁷ R. Wilkinson,²⁵ H. H. Williams,²⁵ P. Wilson,⁵ B. L. Winer,²² D. Winn,¹⁹ D. Wolinski,¹⁹ J. Wolinski,²⁰ S. Worm,²¹ X. Wu,¹⁰ J. Wyss,²⁴ A. Yagil,⁷ W. Yao,¹⁷ K. Yasuoka,³⁵ Y. Ye,¹⁴ G. P. Yeh,⁷ P. Yeh,³² M. Yin,⁶ J. Yoh,⁷ C. Yosef,²⁰ T. Yoshida,²³ D. Yovanovitch,⁷ I. Yu,⁷ L. Yu,²¹ J. C. Yun,⁷ A. Zanetti,²⁶ F. Zetti,²⁶ L. Zhang,³⁷ W. Zhang,²⁵ and S. Zucchelli²

(CDF Collaboration)

¹Argonne National Laboratory, Argonne, Illinois 60439

²Istituto Nazionale di Fisica Nucleare, University of Bologna, I-40127 Bologna, Italy

³Brandeis University, Waltham, Massachusetts 02264

⁴University of California at Los Angeles, Los Angeles, California 90024

⁵University of Chicago, Chicago, Illinois 60638

⁶Duke University, Durham, North Carolina 28708

⁷Fermi National Accelerator Laboratory, Batavia, Illinois 60510

⁸University of Florida, Gainesville, Florida 33611

⁹Laboratori Nazionali di Frascati, Istituto Nazionale di Fisica Nucleare, I-00044 Frascati, Italy

¹⁰University of Geneva, CH-1211 Geneva 4, Switzerland

¹¹Harvard University, Cambridge, Massachusetts 02138

¹²Hiroshima University, Higashi-Hiroshima 724, Japan

¹³University of Illinois, Urbana, Illinois 61801

¹⁴Institute of Particle Physics, McGill University, Montreal, Canada H3A 2T8, and University of Toronto, Toronto, Canada M5S 1A7

¹⁵The Johns Hopkins University, Baltimore, Maryland 21218

¹⁶National Laboratory for High Energy Physics (KEK), Tsukuba, Ibaraki 315 Japan

¹⁷Ernest Orlando Lawrence Berkeley National Laboratory, Berkeley, California 94720

⁸Massachusetts Institute of Technology, Cambridge, Massachusetts 02139

¹⁹University of Michigan, Ann Arbor, Michigan 48109

²⁰Michigan State University, East Lansing, Michigan 48824

²¹University of New Mexico, Albuquerque, New Mexico 87132

²²The Ohio State University, Columbus, Ohio 43220

²³Osaka City University, Osaka 588, Japan

²⁴Universita di Padova, Istituto Nazionale di Fisica Nucleare, Sezione di Padova, I-36132 Padova, Italy

²⁵University of Pennsylvania, Philadelphia, Pennsylvania 19104

²⁶Istituto Nazionale di Fisica Nucleare, University and Scuola Normale Superiore of Pisa, I-56100 Pisa, Italy

²⁷University of Pittsburgh, Pittsburgh, Pennsylvania 15270

²⁸Purdue University, West Lafayette, Indiana 47907

²⁹University of Rochester, Rochester, New York 14628

³⁰Rockefeller University, New York, New York 10021

³¹Rutgers University, Piscataway, New Jersey 08854

³²Academia Sinica, Taipei, Taiwan 11530, Republic of China

³³Texas A&M University, College Station, Texas 77843

³⁴Texas Tech University, Lubbock, Texas 79409

³⁵University of Tsukuba, Tsukuba, Ibaraki 315, Japan

³⁶Tufts University, Medford, Massachusetts 02155

³⁷University of Wisconsin, Madison, Wisconsin 53806

³⁸Yale University, New Haven, Connecticut 06511

(Received 3 February 1997)

We present a study of J/ψ and $\psi(2S)$ production in $p\bar{p}$ collisions, at $\sqrt{s} = 1.8$ TeV with the CDF detector at Fermilab. The J/ψ and $\psi(2S)$ mesons are reconstructed using their $\mu^+\mu^-$ decay modes. We have measured the inclusive production cross section for both mesons as a function of their transverse momentum in the central region, $|\eta| < 0.6$. We also measure the fraction of these events originating from b hadrons. We thus extract individual cross sections for J/ψ and $\psi(2S)$ mesons from b -quark decays and prompt production. We find a large excess (approximately a factor of 50) of direct $\psi(2S)$ production compared with predictions from the color singlet model. [S0031-9007(97)03617-X]

PACS numbers: 13.85.Ni, 14.40.Gx

In high energy $p\bar{p}$ collisions charmonium particles predominantly come from prompt QCD production and the decay of b hadrons [1]. In the color singlet model (CSM), charmonium production begins with the production of a $c\bar{c}$ quark-antiquark pair in a colorless state. The process of forming the bound state preserves the quantum numbers of the initial pair [2]. In this model, J/ψ production is dominated by feeddown from χ_c production. Other sources of prompt J/ψ and $\psi(2S)$ mesons are expected to be negligible. However, we have reported production cross sections for both J/ψ and $\psi(2S)$ mesons at $\sqrt{s} = 1.8$ TeV that are higher than expectations and have a different P_T spectrum [3]. Similarly, measurements of the J/ψ cross section by UA1 [4] at $\sqrt{s} = 0.63$ TeV and the D0 experiment [5] indicate that the measured transverse momentum (P_T) spectrum of J/ψ mesons is not in agreement with predictions for χ_c and b hadron decays alone. In this paper, we use the silicon vertex detector (SVX) in CDF to separate prompt ψ 's [$\psi \equiv J/\psi, \psi(2S)$ in what follows] from ψ 's from b hadron decays. We extract the production cross sections for prompt ψ mesons and find them to be much larger than the CSM predictions.

The CDF detector has been described in detail elsewhere [6]. Muons are reconstructed by matching track segments found in the central muon system (CMU), which covers the region $|\eta| < 0.6$ [7], to charged particle tracks reconstructed in the central tracking chamber (CTC). Approximately 60% of the muon tracks also have hits in the silicon vertex detector which provides measurements in the r - ϕ plane only, resulting in a track impact parameter resolution of $(13 + 40/P_T)$ μm , where P_T (in GeV/c) is the track momentum transverse to the beam line. The data sample consists of $17.8 \pm 0.6 \text{ pb}^{-1}$ of $p\bar{p}$ collisions at $\sqrt{s} = 1.8$ TeV from the 1992–1993 data taking period, collected using dimuon triggers in the CDF three-level trigger system. The level 1 dimuon trigger requires two track segments in the CMU, separated by at least 5° in azimuth. The trigger efficiency for each muon at level 1 rises from 50% at $P_T = 1.6 \text{ GeV}/c$ to 90% at $P_T = 3.1 \text{ GeV}/c$ with a plateau of 94%. The level 2 trigger requires that at least one of the muon track segments is matched in ϕ to a track found in the CTC by the central fast tracker (CFT) [8], a hardware track-finding processor. The efficiency for finding a track with the CFT rises from 50% at $P_T = 2.7 \text{ GeV}/c$ to 90% at $P_T = 3.1 \text{ GeV}/c$ and reaches a plateau of 93%. The level 3 trigger requires a pair of oppositely charged muons after full track reconstruction.

A period with reduced level 3 tracking efficiency is excluded from the J/ψ analysis where the data sample is large, but is included in the $\psi(2S)$ analysis with a correction derived from the J/ψ sample. The considered integrated luminosity in the J/ψ sample is limited to $15.4 \pm 0.6 \text{ pb}^{-1}$. When the fraction of ψ 's from b decays is measured, an additional $\sim 90 \text{ pb}^{-1}$ of data from the 1994–1995 collider run is added to the sample. This data sample is not included in the cross section measure-

ment because the trigger and reconstruction efficiencies are still under study.

Reconstructed muons are required to have CMU hits consistent with the CTC track. The CTC track is extrapolated to the CMU chambers and is required to lie within 3σ of the CMU hits, where σ is the uncertainty in the extrapolated position due to multiple scattering. The calorimeter tower in front of the muon chamber segment is required to have nonzero energy deposition. To remain in the region of good trigger efficiency, both muons are required to have $P_T > 2.0 \text{ GeV}/c$, and one muon is required to have $P_T > 2.8 \text{ GeV}/c$. The two muon tracks are fit with the requirement that they originate from a common point. We require that the one degree-of-freedom fit have $\chi^2 < 10$. Where available, we use SVX information to improve the track measurement. To remain in the region of good acceptance to ψ decays, the ψ candidate is required to satisfy $|\eta| < 0.6$ and $P_T > 5 \text{ GeV}/c$. There are approximately 22 100 J/ψ and 800 $\psi(2S)$ candidates over a background of 1000 events in a mass window of $80 \text{ MeV}/c^2$.

The number of ψ candidates in the data is determined by fitting the $\mu^+\mu^-$ invariant mass distribution with templates generated from Monte Carlo simulation of $\psi \rightarrow \mu^+\mu^-$ decays. The Monte Carlo includes the small distortions to the $\mu^+\mu^-$ mass spectrum arising from $\psi \rightarrow \mu^+\mu^-\gamma$ final states. The muon momenta are smeared to simulate the detector resolution. Since the resulting $\mu^+\mu^-$ invariant mass resolution is a function of the transverse momentum of the ψ , the data are fit separately in each bin in $P_T(\psi)$. To correct for the trigger efficiency ($\epsilon_{\text{trigger}}$), which is a function of the P_T of both muons, each event is weighting by $1/\epsilon_{\text{trigger}}$, and the mass distribution is fit to the signal shape fixed from the simulation plus a linear background. The fits have very good quality in all P_T bins, with a χ^2 per degree of freedom ranging from 0.5 to 1.5. The width of the mass peak rises from 17 to 35 MeV/c^2 for $P_T(\psi)$ in the range 5–20 GeV/c .

The ψ differential cross section is defined by

$$\frac{d\sigma(\psi)}{dP_T} \mathcal{B}(\psi \rightarrow \mu^+\mu^-) = \frac{N(\psi)}{\epsilon \int \mathcal{L} dt \cdot \Delta P_T},$$

where $N(\psi)$ is the number of ψ candidates in the bin corrected for trigger efficiency, $\int \mathcal{L} dt$ is the integrated luminosity, ΔP_T is the size of the P_T bin, and ϵ is the product of the detector and kinematic acceptance, the efficiencies of the event reconstruction and event selection requirements, whereas $\mathcal{B}(\psi \rightarrow \mu^+\mu^-)$ is the branching fraction for the decay $\psi \rightarrow \mu^+\mu^-$.

The acceptance is determined from Monte Carlo simulation. ψ events are generated with a flat distribution in P_T , η , and ϕ . A parametrized detector simulation is used, and the kinematic requirements are then applied to the generated events. The acceptance is found to rise from 9% at $P_T(\psi) = 5 \text{ GeV}/c$ to a plateau value of 28% for

$P_T(\psi) > 14 \text{ GeV}/c$. The acceptance also depends on the ψ polarization. Taking θ^* to be the angle between the ψ direction in the lab frame and the μ^+ direction in the ψ rest frame, the angular distribution of the decay will have the form $1 + \alpha \cos^2 \theta^*$, where α ($-1 \leq \alpha \leq 1$) describes the polarization of the parent ψ . The magnitude of the uncertainty on the ψ acceptance will be different for prompt ψ 's and ψ 's from b hadron decays. Prompt ψ 's can in principle be fully polarized. From a Monte Carlo simulation of b hadron decays, we estimate that a ψ hadron with a polarization of +1 (-1) in the b hadron rest frame will have an effective polarization of only 0.143 (-0.219) in the ψ rest frame. We assign half of the maximum change in the acceptance (corresponding to changing α between -1 and +1) in each P_T bin as the uncertainty in each case. This uncertainty varies with $P_T(\psi)$, from 15% of the acceptance at $P_T(\psi) = 5 \text{ GeV}/c$ to 5% (of the acceptance) at $P_T(\psi) = 20 \text{ GeV}/c$ for prompt production. The respective uncertainty for the cross section from b hadron decays decreases from 6% to 3% in the same $P_T(\psi)$ range.

The efficiency of the CMU segment reconstruction is measured using dimuon events recorded with a single muon trigger to be $97.2 \pm 1.2\%$. The efficiency of the CTC track reconstruction is measured by embedding hits from Monte Carlo simulated particle tracks in data events, and attempting to reconstruct the added track. This efficiency is found to depend on the number of tracks near the embedded track. Only approximately 3% of the data have tracks where the efficiency to find the track is less than its plateau value of 98.4%. The average efficiency for reconstructing both CTC tracks is $96.4 \pm 2.8\%$. The efficiency of the CMU-CTC matching requirements is estimated from the number of J/ψ events before and after the matching requirements. The requirements are $90.5 \pm 1.0\%$ efficient.

Systematic uncertainties on the trigger efficiency are estimated by varying the functional form of the trigger efficiency, which is determined from dimuon events recorded with a single-muon trigger. Variation of the level 1 trigger efficiency parametrization causes an uncertainty of 6.4% (6.1%) in the integrated J/ψ [$\psi(2S)$] cross sections. Similarly, there is a 1.1% (1.0%) systematic uncertainty in the J/ψ [$\psi(2S)$] cross section from the level 2 trigger efficiency. Finally, the level 3 trigger efficiency was estimated by examining the number of reconstructed muons found by the on-line requirements. These requirements are less efficient in the runs excluded from the J/ψ analysis, resulting in different efficiencies for the two states. The J/ψ efficiency is $97.0 \pm 0.2\%$, and the $\psi(2S)$ efficiency is $92.3 \pm 0.2\%$.

The integrated cross sections are

$$\sigma(J/\psi)\mathcal{B}(J/\psi \rightarrow \mu^+\mu^-) = 17.4 \pm 0.1(\text{stat})_{-2.8}^{+2.6} \text{ (syst) nb,}$$

$$\sigma[\psi(2S)]\mathcal{B}[\psi(2S) \rightarrow \mu^+\mu^-] = 0.57 \pm 0.04(\text{stat})_{-0.09}^{+0.08} \text{ (syst) nb,}$$

where $\sigma(\psi) \equiv \sigma(p\bar{p} \rightarrow \psi X, P_T(\psi) > 5 \text{ GeV}/c, |\eta(\psi)| < 0.6)$.

We extract the fraction of ψ 's that originate from b hadrons using ψ candidates with both muons reconstructed in the SVX. The two muons are constrained to come from the same point which we refer to as the secondary vertex, to be distinguished from the primary vertex in the event. We measure the projection of the decay length onto the ψ transverse momentum, L_{xy} . This is converted into the proper lifetime of the assumed b hadron parent by $c\tau = L_{xy}/[P_T(\psi)/m(\psi)F_{\text{corr}}]$, where $m(\psi)$ is the mass of the ψ state and F_{corr} is a correction factor, estimated from Monte Carlo simulations, that relates the boost factor $\beta\gamma$ of the ψ to the boost factor of the parent b hadron. Details of this procedure can be found in the measurement of the average b hadron lifetime [9].

The prompt component of the signal is parametrized by the resolution function, centered at $c\tau = 0$. The component of the signal due to b hadron decays is represented by an exponential of lifetime $c\tau_b$, convoluted with the resolution function. In this analysis we remove all track selection requirements described in [9] that may potentially affect the isolation of the ψ meson and thus the extracted fraction of ψ 's originating from b hadrons. As a result, the resolution function is augmented with two additional exponential tails. The tails constitute about 2% of the total number of candidates. We fix $c\tau_b$ to 438 μm , as found by the CDF inclusive b hadron lifetime measurement [9]. The lifetime and normalization of the remaining exponentials are left as free parameters in the fit.

The data $c\tau$ distribution is fit in each $P_T(\psi)$ bin using an unbinned log-likelihood fit. The background fraction in the signal region is allowed to vary within the uncertainty in the normalization extracted from the ψ sidebands. The resulting fraction of ψ candidates originating from b hadron decays, $f_b(P_T)$, is shown as a function of $P_T(\psi)$ in Fig. 1. Several variations in the fitting technique produced an average relative variation of $\pm 0.9\%$, a value taken to be the systematic uncertainty on f_b due to the fitting procedure. Varying the average b hadron lifetime by 1 standard deviation changes f_b by $\pm 0.7\%$.

In order to minimize the effects of statistical fluctuations, a χ^2 fit is performed on $f_b(P_T)$. The fitted function is the average value of a parabola, weighted by the observed shape of the cross section.

The cross section for ψ 's from b hadron decays is extracted by multiplying the fitted fraction $f_b^{\text{fit}}(P_T)$ with the inclusive ψ production cross section. The cross sections for ψ 's from b hadron decays are shown in Fig. 2. The theoretical predictions were calculated by generating b quarks according to the next-to-leading order (NLO) QCD predictions [10], using a scale $\mu = \mu_0 \equiv \sqrt{m_b^2 + P_T^2}$ and $m_b = 4.75 \text{ GeV}/c^2$. The b quark is fragmented into b hadrons using Petersen fragmentation [11] with the fragmentation parameter, ϵ_b , set to 0.006. The b hadron is decayed to a ψX with a parametrization

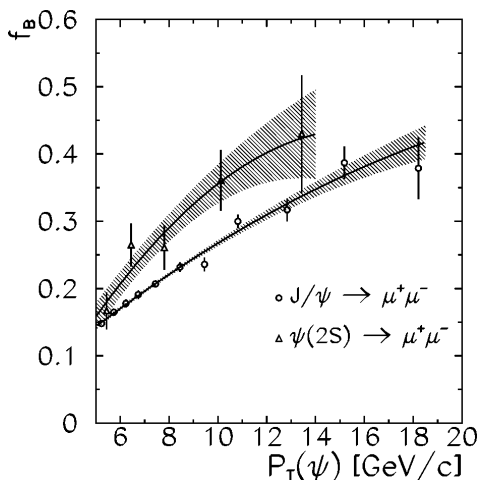


FIG. 1. The fractions of J/ψ (circles) and $\psi(2S)$ (triangles) originating from b -hadron decays. The error bars indicate the combined statistical and systematic uncertainties on the fractions. The solid curve is the fitted function, and the slashed regions indicate the uncertainty in the fit.

of the momentum distribution measured by the CLEO experiment [12]. Details of this procedure can be found in Ref. [13]. The data are higher than the QCD prediction by a factor of 3–4 depending on $P_T(\psi)$. The uncertainty in the theoretical cross section (shown as the dashed and dotted curves in Fig. 3) is estimated by varying the scale μ to $\mu_0/4$ and $2\mu_0$ and ϵ_b to 0.004 and 0.008.

Multiplying the inclusive ψ cross section with the factor $(1 - f_b^{\text{fit}})$ results in the cross section for prompt ψ production, displayed in Fig. 3. Both cross sections are higher than theoretical predictions based on the color singlet model [14] by a factor of ~ 6 for J/ψ 's and a factor of ~ 50 for $\psi(2S)$. In the case of $\psi(2S)$ mesons, where the transition $\chi_c \rightarrow \psi(2S)$ is kinematically forbidden, the interpretation of this prompt component is straightforward, as being due to direct $\psi(2S)$ production. In the case of J/ψ production, one must deconvolute various sources of prompt J/ψ mesons: the $\psi(2S) \rightarrow J/\psi$ transition, the $\chi_c \rightarrow J/\psi$ transition, and direct J/ψ production. A measurement from the $\chi_c \rightarrow J/\psi\gamma$ transition is described in [15]. A recent model that attempts to explain this discrepancy with theoretical expectations is the color octet model [16]. In this model, the shape of the cross section as a function of $P_T(\psi)$ is calculated perturbatively. However, the normalization depends on nonperturbative matrix elements for which there exist only an order of magnitude predictions. These amplitudes can in principle be measured by fitting the shapes calculated in [16] to the data.

In conclusion, we have measured the inclusive J/ψ and $\psi(2S)$ production cross sections. We have separated prompt ψ 's from ψ 's originating from b hadron decays. The b component is a factor of 3–4 higher than theoretical predictions. The prompt component is also higher than expectations from the color singlet model. For $\psi(2S)$

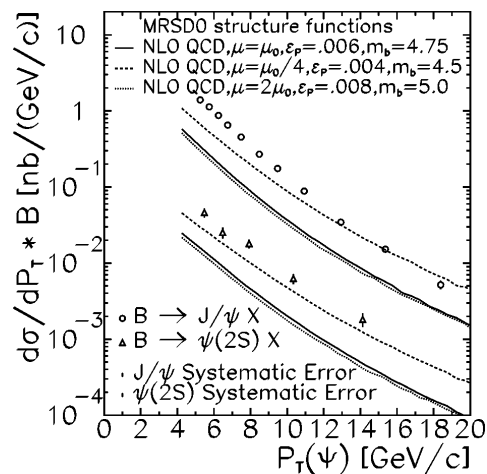


FIG. 2. The differential cross section times branching ratio $B(\psi \rightarrow \mu^+\mu^-)$ for $|\eta^\psi| < 0.6$ for ψ mesons originating from b hadron decays. The solid lines indicate the theoretical predictions based on perturbative QCD. The dashed and dotted lines are based on the same calculation with the QCD scale, the mass of the b quark and the Petersen fragmentation parameter varied within their uncertainties.

mesons, the prompt data are more than an order of magnitude higher (approximately a factor of 50) than the theoretical calculations. A possible explanation for this very large excess may come from the color octet model introduced recently.

We thank the Fermilab staff and the technical staffs of the participating institutions for their vital contributions. This work was supported by the U.S. Department of Energy and National Science Foundation, the Italian Istituto Nazionale di Fisica Nucleare, the Ministry of Education, Science and Culture of Japan, the Natural

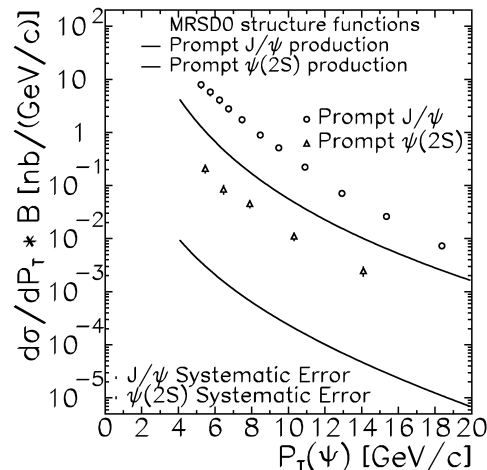


FIG. 3. The differential cross section times branching ratio $B(\psi \rightarrow \mu^+\mu^-)$ for $|\eta^\psi| < 0.6$ for prompt ψ mesons. The vertical error bars are the statistical and the P_T -dependent systematic uncertainties, added in quadrature. Circles: J/ψ ; triangles: $\psi(2S)$. The lines are the theoretical expectations based on the color singlet model.

Sciences and Engineering Research Council of Canada, the National Science Council of the Republic of China, and the A. P. Sloan Foundation.

*Visitor.

- [1] E. W. N. Glover, A. D. Martin, and W. J. Stirling, *Z. Phys. C* **38**, 473 (1988).
- [2] R. Baier and R. Ruckl, *Z. Phys. C* **19**, 251 (1983).
- [3] CDF Collaboration, F. Abe *et al.*, *Phys. Rev. Lett.* **69**, 3704 (1992).
- [4] UA1 Collaboration, C. Albajar *et al.*, *Phys. Lett. B* **256**, 121 (1991).
- [5] D0 Collaboration, S. Abachi *et al.*, *Phys. Lett. B* **370**, 239 (1996).
- [6] CDF Collaboration, F. Abe *et al.*, *Nucl. Instrum. Methods Phys. Res., Sect. A* **271**, 376 (1988), and references therein. The silicon vertex detector is described in CDF Collaboration, F. Abe *et al.*, *Phys. Rev. D* **50**, 2966 (1994).
- [7] In CDF, the positive z axis lies along the proton direction, r is the radius from this axis, θ is the polar angle, and ϕ is the azimuthal angle. The pseudorapidity, η , is defined as $-\ln[\tan(\theta/2)]$.
- [8] G. W. Foster *et al.*, *Nucl. Instrum. Methods Phys. Res., Sect. A* **269**, 93 (1988).
- [9] CDF Collaboration, F. Abe *et al.*, *Phys. Rev. Lett.* **71**, 3421 (1993).
- [10] P. Nason, S. Dawson, and R. K. Ellis, *Nucl. Phys.* **B327**, 49 (1988).
- [11] C. Petersen *et al.*, *Phys. Rev. D* **27**, 105 (1983).
- [12] CLEO Collaboration, R. Balest *et al.*, in Proceedings of the 27th International Conference on High-Energy Physics, Glasgow, Scotland, 1996 (Report No. GLS0248).
- [13] T. Daniels, Ph.D. dissertation, Massachusetts Institute of Technology, 1997.
- [14] E. Braaten, M. A. Doncheski, S. Fleming, and M. L. Mangano, *Phys. Lett. B* **333**, 548 (1994); M. Cacciari and M. Greco, *Phys. Rev. Lett.* **73**, 1586 (1994).
- [15] CDF Collaboration, F. Abe *et al.*, following Letter, *Phys. Rev. Lett.* **79**, 578 (1997).
- [16] E. Braaten and S. Fleming, *Phys. Rev. Lett.* **74**, 3327 (1995); P. Cho and M. Wise, *Phys. Lett. B* **346**, 129 (1995); M. Cacciari, M. Greco, M. L. Mangano, and A. Petrelli, *Phys. Lett. B* **356**, 553 (1995); P. Cho and A. K. Leibovich, *Phys. Rev. D* **53**, 150 (1996); P. Cho and A. K. Leibovich, *Phys. Rev. D* **53**, 6203 (1996).